

## Optimal Parametric Feedback Excitation of Nonlinear Oscillators

David J. Braun\*

Singapore University of Technology and Design, 8 Somapah Road, 487372 Singapore

(Received 14 July 2015; published 28 January 2016)

An optimal parametric feedback excitation principle is sought, found, and investigated. The principle is shown to provide an adaptive resonance condition that enables unprecedentedly robust movement generation in a large class of oscillatory dynamical systems. Experimental demonstration of the theory is provided by a nonlinear electronic circuit that realizes self-adaptive parametric excitation without model information, signal processing, and control computation. The observed behavior dramatically differs from the one achievable using classical parametric modulation, which is fundamentally limited by uncertainties in model information and nonlinear effects inevitably present in real world applications.

DOI: 10.1103/PhysRevLett.116.044102

Parametric resonance was first reported by Faraday in 1831 [1]; he observed surface waves in a fluid-filled cylinder under vertical excitation exhibiting half the frequency of the excitation. One of the simplest mathematical models that explains this effect is given by the (damped) Mathieu equation [2]:  $\ddot{q} + \gamma\dot{q} + [\omega_0^2 + \epsilon \cos(\omega_p t)]q = 0$ . Under weak excitation and small dissipation this *linear* oscillator displays an instability effect, provided the natural frequency is near half the frequency of the excitation  $\omega_0/\omega_p \approx 1/2$  and the excitation strength is above the instability threshold  $\epsilon/\omega_p > \gamma$  [3].

*Nonlinear* oscillators, in general, do not exhibit unbounded behavior under parametric excitation (even if there is no dissipation) [4]. This is because nonlinearity relates the amplitude and the frequency of the oscillator; when the amplitude increases, the natural frequency changes, i.e., *detunes* with respect to the constant frequency of the excitation [5]. This effect imposes a fundamental limit to many practical applications aiming to achieve large amplitude oscillations [6,7]. One of the main reasons for this limitation stems from parametric excitation realized in a feed-forward manner, using nonadaptive time-dependent fixed-frequency modulation.

In this Letter, we propose an alternative means to parametric excitation using optimal feedback perturbations. Application of this idea converts a parametrically modulated nonautonomous oscillator to a feedback controlled hybrid state automaton. As opposed to time-dependent feed-forward excitation, the proposed state-dependent modulation is not affected by nonlinearity induced amplitude saturation, and is shown to provide robust movement amplification for both undamped linear and damped nonlinear oscillators. Compared to time-delay feedback control [8]—used in wide variety of applications to realize direct forcing [9] as well as parametric modulation [10–13]—our controller employs instantaneous state feedback to implement an optimization-based adaptive resonance condition without model information, sophisticated on-line

computation, continuous measurements, or signal processing (frequency and phase identification) from past observations. In this way, it provides an *effective* and *robust* mechanism to parametric excitation desirable in practical applications.

*Example.*—To motivate the derivation of our feedback controller we will first consider a canonical optimal control problem with an aim to maximize the displacement  $q(t)$  of a harmonic oscillator using stiffness modulation

$$\max_{(u,T) \in \mathbb{U} \times \mathbb{R}^+} |q(T) - q(0)| \quad (1)$$

$$\text{subject to } \ddot{q} + k(u)q = 0, \quad q(0) \neq 0, \quad \dot{q}(0) = 0,$$

where  $k = k(u) > 0$  is the control dependent stiffness,  $\mathbb{U} = [u_{\min}, u_{\max}]$  is the admissible control space, while  $T$  is a finite but otherwise unspecified terminal time. Under a relatively weak technical assumption [i.e.,  $dk(u)/du > 0$ ], the optimal feedback controller to the above problem is given by

$$u_{\text{FB}}^{\text{opt}}(q, \dot{q}) \in \begin{cases} u_{\max} & \text{if } q\dot{q} \leq 0 \\ u_{\min} & \text{if } q\dot{q} > 0. \end{cases} \quad (2)$$

Application of this control law on the oscillator (1) {i.e.,  $\ddot{q} + k[u_{\text{FB}}^{\text{opt}}(q, \dot{q})]q = 0$ } leads to movement amplification according to the following recurrence relation:  $q_{n+1} = \lambda_{\text{FB}}^{\text{opt}} q_n$ , where  $q_n = q(nT)$  indicates the amplitude of the oscillator,  $n \in \mathbb{N}$  denotes the number of motion cycles,  $T = \pi[k_{\min}^{-(1/2)} + k_{\max}^{-(1/2)}]$  is the time required for one cycle during the oscillations while  $\lambda_{\text{FB}}^{\text{opt}} = k_{\max}/k_{\min}$  is the cycle-to-cycle amplitude ratio. Evidently, if  $\lambda_{\text{FB}}^{\text{opt}} > 1$ , the amplitude of the oscillator will grow without bound over time. Notably, the above optimization suggests a bang-bang type state dependent stiffness modulation for the most effective movement generation [14].

The controller presented above can be derived by the following static optimization:  $\max_{u \in \mathbb{U}} -k(u)\dot{q}$ . As

suggested by this formulation, the above dynamic optimization implements instantaneous power maximization. In this Letter we adapt the idea of instantaneous power maximization to realize dynamically optimal movement generation for damped nonlinear oscillators. This idea is the subject of the following generalization.

*Parametric feedback controller.*—Let us now consider a nonlinear oscillator

$$\ddot{q} + \gamma \dot{q} = F(q, u), \quad (3)$$

where  $\gamma \geq 0$  characterizes dissipation, the system has an equilibrium at  $q = q_o$ , i.e.,  $\forall u: F(q_o, u) = 0$ , the force  $F(q, u)$  is a symmetric function of the oscillators displacement, i.e.,  $-F(q - q_o, u) = F(-(q - q_o), u)$  and it is restoring at large displacements, i.e.,  $\forall (|q - q_o| \gg 1, u): F(q - q_o, u)(q - q_o) < 0$ . Below, we shall find convenient to represent this force in the following form:

$$F(q, u) = -K(q, u)(q - q_o), \quad (4)$$

where for small displacements  $K(q \approx q_o, u) = k_1(u) = -\partial F / \partial q|_{q=q_o}$  is the *local* stiffness that characterizes the stability of the equilibrium  $q_o$ , while for large displacements  $K(q, u) > 0$  is a *global* stiffness that indicates the extent to which the force acts towards the equilibrium. In the following, we introduce an optimal feedback controller for movement amplification using nonlinear parametric excitation.

Consider a dynamical system (3) and (4) where the control input is chosen to maximize the power input to the oscillator according to the following static optimization:

$$\max_{u \in \mathbb{U}} -K(q, u)(q - q_o)\dot{q}. \quad (5)$$

Assuming that (i) the global stiffness  $K = K(q, u)$  is a strictly monotonic function of the control input  $u \in \mathbb{U}$  and that (ii) the admissible control space is given by a box constraint  $\mathbb{U} = [u_{\min}, u_{\max}]$ , the feedback controller predicted by the above optimization is given by the following relation:

$$u_{\text{FB}}^{\text{opt}}(q, \dot{q}) \in \begin{cases} u_{\max} & \text{if } s(q, \dot{q}) < 0 \\ \mathbb{U} & \text{if } s(q, \dot{q}) = 0 \\ u_{\min} & \text{if } s(q, \dot{q}) > 0, \end{cases} \quad (6)$$

where  $s(q, \dot{q}) = \text{sgn}(\partial K / \partial u)(q - q_o)\dot{q}$  is the switching function. It turns out that under relatively weak technical assumptions [i.e.,  $F(q, u)$  and  $\partial F(q, u) / \partial q$  are continuous for all admissible positions and controls], the optimality condition asserted by Pontryagin's maximum principle [15] to an associated dynamic optimization—where the goal is

to maximize the amplitude of the damped nonlinear oscillator (3) and (4) at each oscillation—is equivalent to (6); see Ref. [16]. This is to say that the nonlinear parametric excitation (6), derived from the static optimization (5), implements a dynamically optimal strategy to amplitude maximization on a large class of damped nonlinear oscillators.

There are a number of notable features to the proposed controller (6): first it is state dependent and as such more robust than an alternative time-dependent feed-forward controller; second, it does not require model information to be implemented; and, third, it is a switching controller that can be operated without continuous sensory feedback. Furthermore, the two assumptions in the derivation of (6) are rather general, i.e., they can be satisfied by a wide class of physical mechanisms used to implement parameter modulation in different physical domains and scales [4,6,11–13]. Finally, we note that the proposed controller does not guarantee movement amplification; i.e., in order to provide movement amplification, the energy injected through parametric excitation should exceed the amount of energy being dissipated [16]. Below we shall demonstrate this under fairly general conditions in simulation and experimental implementation.

*Application.*—At first glance we aim to test the robustness and efficacy of the proposed controller when applied to a damped linear oscillator:

$$\ddot{q} + \gamma \dot{q} + k_1(u)q = 0, \quad (7)$$

where  $\gamma \geq 0$  characterizes dissipation,  $k_1(u) = 1 + \Delta k u \in [k_{1\min}, k_{1\max}]$  is a positive control dependent stiffness, while  $u \in \mathbb{U} = [-1, 1]$  is the control input. Application of the proposed feedback controller (6) on this system leads to the following recurrence relation:

$$q_{n+1} = \lambda_{\text{FB}}^{\text{opt}}(\gamma, \Delta k) q_n = \frac{k_{1\max}}{k_{1\min}} e^{-(1/2)\gamma T} q_n,$$

where  $q_n = q(nT)$  is the amplitude of the oscillator,  $n$  denotes the number of motion cycles,  $T = \omega_+^{-1}(\pi + 2\varphi_+) + \omega_-^{-1}(\pi - 2\varphi_-)$  is the time required for one motion cycle,  $\omega_{\pm}^2 = 1 \pm \Delta k - \frac{1}{4}\gamma^2$  is the squared angular velocity,  $\varphi_{\pm} \in [0, \pi/2)$  is the phase implicitly given by  $\tan(\varphi_{\pm}) = \frac{1}{2}\gamma\omega_{\pm}^{-1}$ , while  $\lambda_{\text{FB}}^{\text{opt}}$  is the cycle to cycle amplitude ratio. The region in the parameter space  $\lambda_{\text{FB}}^{\text{opt}}(\gamma, \Delta k) > 1$ , leading to parametric resonance, is shown in Fig. 1(a) (shaded area).

As an alternative means to amplification, one may utilize feed-forward modulation. Among all continuous and piecewise-continuous excitations, including but not limited to resonant sine wave  $u_{\text{FF}}^{\text{sin}} = \sin(4\pi t/T)$  and square wave  $u_{\text{FF}}^{\text{sqw}} = \text{sgn}[\sin(4\pi t/T)]$  modulations [2,18], the following, when perfectly tuned, i.e.,  $\delta k = 0$ ,

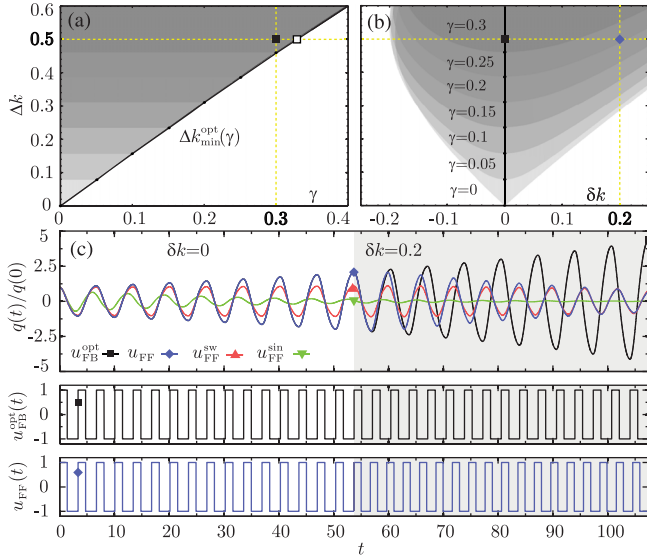


FIG. 1. (a)  $(\gamma, \Delta k)$  stability chart for the damped linear oscillator (7) under optimal parametric feedback control. The resonance condition is given by  $\Delta k > \Delta k_{\min}^{\text{opt}}(\gamma) = \frac{1}{2}\pi\gamma - [(3/16)\pi - (1/192)\pi^3]\gamma^3 + O(\gamma^5)$ . (b)  $(\delta k, \Delta k; \gamma)$  stability chart showing the behavior of the oscillator under perfectly tuned ( $\delta k = 0$ ) and off-tuned ( $\delta k \neq 0$ ) feed-forward modulation (8). (c) Behavior of the oscillator ( $\gamma = 0.3$ ,  $\Delta k = 0.5$ ) under optimal feedback excitation, feed-forward modulation, square wave modulation, and sine wave modulation under perfectly tuned conditions ( $\delta k = 0$ , white area) and when off-tuning is present ( $\delta k = 0.2$ , shaded area). The effectiveness and robustness of the feedback controller is evident from these simulations.

$$u_{\text{FF}}(t; \gamma, \Delta k, \delta k) \in \begin{cases} 1 & \text{if } t \in [nT, nT + T_+) \\ -1 & \text{if } t \in [nT + T_+, nT + T_+ + T_-) \\ 1 & \text{if } t \in [nT + T_+ + T_-, nT + 2T_+ + T_-) \\ -1 & \text{if } t \in [nT + 2T_+ + T_-, nT + 2T_+ + 2T_-), \end{cases} \quad (8)$$

where  $T_{\pm} = \Omega_{\pm}^{-1}[(\pi/2) + \Phi_{\pm}]$ ,  $\Omega_{\pm}^2 = \omega_{\pm}^2 + \delta k$ ,  $\tan(\Phi_{\pm}) = \frac{1}{2}\gamma\Omega_{\pm}^{-1}$ , leads to the most effective amplification. The amplification rate of the corresponding optimal feed-forward controller,  $u_{\text{FF}}^{\text{opt}} = u_{\text{FF}}(t; \gamma, \Delta k, 0)$ , is the same as the one obtained using the proposed feedback controller, and under perfect knowledge of the system parameters the two controllers would indeed perform the same [Fig. 1(c), white area]. However, there is a crucial difference between these two controllers in applications when system parameters are not precisely identifiable. This is because unlike the feed-forward controller, the feedback controller is able to adapt both the frequency and the phase of the excitation according to the changes in behavior of the oscillator. This is what makes our parametric excitation independent of the constraint imposed by the limited mistuning [19] allowable

during feed-forward modulation [Figs. 1(b) and 1(c), shaded areas].

We will now investigate the effect of nonlinearity on the behavior of the proposed controller. For this purpose, let us consider a prototypical parametrically controlled oscillator,

$$\ddot{q} + k_1(u)q + k_3q^3 = 0, \quad (9)$$

where  $k_1(u) = k_0 + \Delta ku \in [k_{1\min}, k_{1\max}]$  is the control dependent stiffness,  $u \in \mathbb{U} = [-1, +1]$  is the control input, while  $k_3 > 0$  introduces Duffing-type nonlinearity [20]. It is known that a typical Duffing nonlinearity results in amplitude saturation under fixed frequency excitation (e.g., sine-wave and square-wave stiffness modulation) even under no dissipation [4,5,7]. However, when the oscillator above is subject to the proposed parametric feedback excitation, its amplitude approaches infinity (from almost all initial conditions) even under infinitesimally small excitation [16]:

$$q_{n \rightarrow \infty}^2 \sim \frac{k_{1\max} - k_{1\min}}{k_3} n, \quad (10)$$

where  $q_n$  denotes the amplitude at every half motion cycle. This is to say that the proposed feedback controller is not prone to the classical limitation known as amplitude saturation due to nonlinearity induced frequency detuning. This is because it automatically adapts the frequency (and the phase) of the excitation based on the behavior of the oscillator (see Fig. 2).

For the considered undamped system (9), the prediction given by (10) is valid not only for the monostable case [ $0 \leq k_{1\min} < k_{1\max}$ , see Fig. 2(a)] but also when the oscillator displays bistable behavior [ $k_{1\min} < 0 \leq k_{1\max}$  or  $k_{1\min} < k_{1\max} < 0$  as shown in Fig. 2(b)]. However, the long term behavior of such a nonlinear oscillator can be much more complicated when damping is not negligible. Notably, in addition to the finite amplitude oscillations in the monostable case and the sustained large amplitude interwell oscillations in the presence of bistability, we may also observe bifurcation leading to off-centered intrawell oscillations when the system is weakly excited and operated in the bistable regime. These qualitatively different behaviors have been observed in our experimental implementation.

*Implementation.*—Laboratory experiments have been carried out to demonstrate the feasibility of the present parametric feedback control scheme under real-world conditions. The electronic circuit [Fig. 3(a)] used in these experiments is a damped nonlinear oscillator. Depending on the externally adjustable static stiffness parameter  $V_{k_0}$ , this circuit can emulate a *monostable* oscillator—characterized with a single-well static potential—or a *bistable* oscillator—characterized with a double-well potential. The corresponding static bifurcation diagram, showing the location of the equilibrium points in a function of  $V_{k_0}$ ,

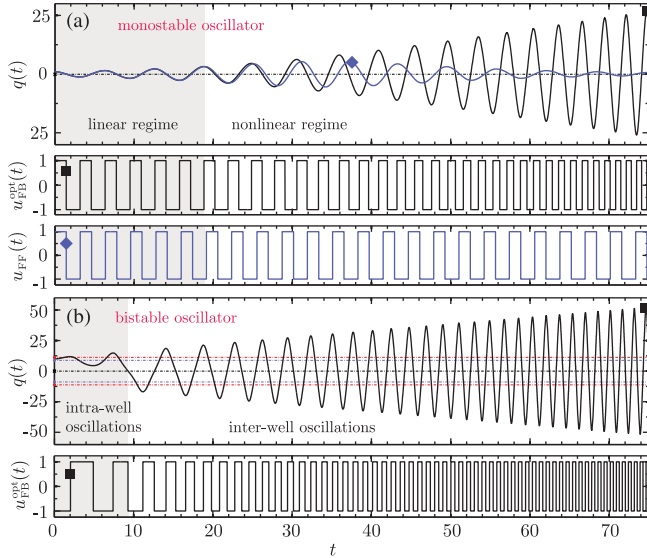


FIG. 2. (a) Monostable Duffing oscillator (9) ( $k_0 = 1$ ,  $k_3 = 0.01$ ,  $\Delta k = 0.2$ ) under optimal parametric feedback control. No model parameters are used to implement this controller. The same plot also shows the behavior of the oscillator under feed-forward parametric excitation implemented using the model-based controller  $u_{FF}(t; \gamma = 0, \Delta k = 0.2, \delta k = 0)$  (8). This controller is optimal in the present context under the assumption that the nonlinearity is negligible, i.e.,  $k_3 \approx 0$ . (b) Bistable Duffing oscillator ( $k_0 = -1$ ,  $k_3 = 0.01$ ,  $\Delta k = 0.2$ ) under optimal parametric feedback control. The dotted lines denote the location of the stable nontrivial and the unstable trivial equilibrium positions of the system (i.e., when  $u = u_{\max}$  and  $u = u_{\min}$ ). Self-tuning of the excitation is evident for the feedback control implementation.

is depicted in Fig. 3(b) ( $V_{\Delta k} = 0$ ). Figure 3(c) shows the behavior of this circuit in strongly nonlinear (bistable) regimes under low amplitude and high amplitude parametric modulation. The corresponding self-adaptive parameter modulation is shown in Fig. 3(d). The experimental data illustrate the qualitatively different behaviors of the weakly excited oscillator [Figs. 3(b), 3(c), left] as well as the robust large amplitude interwell motion of the oscillator under strong excitation [Figs. 3(b), 3(c), right]. These results corroborate the theoretical arguments outlined above, in particular, the efficacy of the controller in movement amplification and its ability to self-tune against substantial unforeseen parameter variation. The observed behavior dramatically differs from the one achievable using feed-forward parametric excitation that, aside from being limited in nonlinear domains, would require retuning in practical implementation.

Our implementation is subject to a number of practical effects not present in the above consideration. Most notably, these are due to (i) design imperfections—resulting in symmetry breaking terms in the restoring force [22], (ii) feedback delay—induced by a practical, dual threshold noise-immunized realization of the switching automaton (implemented using a Schmitt trigger comparator [23]), and

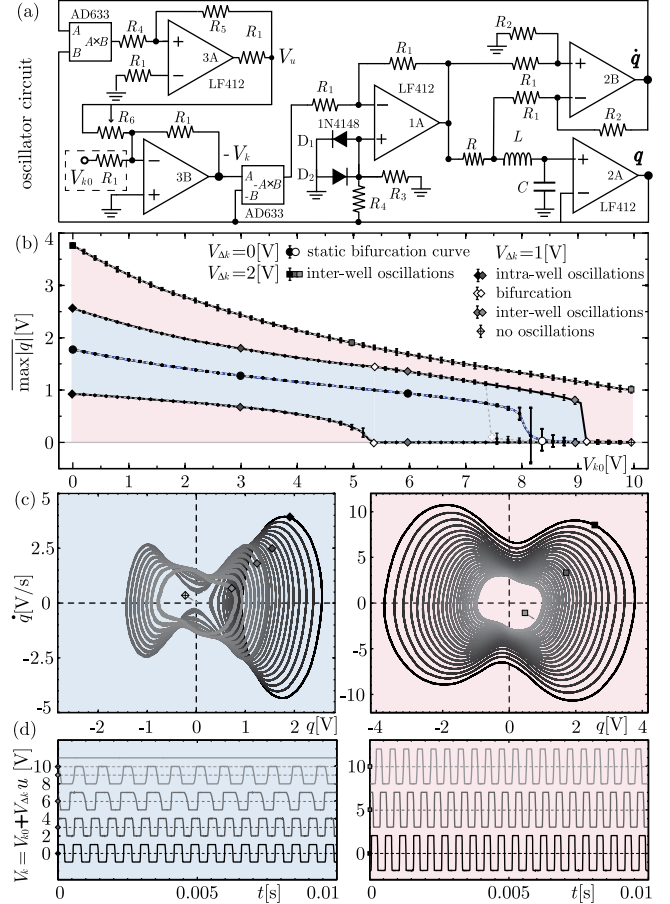


FIG. 3. (a) Tunable parametrically excited nonlinear oscillator  $\ddot{q} + \gamma \dot{q} = F(q, u)$ . The force function is given by  $F(q, u) = F_D(q) + F_{PE}(q, u)$ , where the first term (implemented with diodes  $D_{1,2}$ ) resembles the bistable Silva-Young oscillator [21] while the second term  $F_{PE}(q, u) = -(k_0 + \Delta k u)q = -\alpha V_k(u)q = -\alpha(V_{k0} + V_{\Delta k} u)q$  (where  $\alpha$  is a circuit parameter) provides parametric excitation. The controller (6),  $u = V_u/V_{u\max} = u_{FB}^{\text{opt}}(q, \dot{q})$ , is implemented using a Schmitt trigger comparator. The amplitude of the parametric excitation  $V_{\Delta k} \propto R_1/R_6$  is adjusted by  $R_6$ . Further, we use an external input  $V_{k0}$  to change the static stiffness of this circuit. The values of the analog components are  $L = 12$  mH,  $C = 470$  nF,  $R = 10$   $\Omega$ ,  $R_1 = 10$  k $\Omega$ ,  $R_2 = 1$  M $\Omega$ ,  $R_3 = 1.5$  k $\Omega$ ,  $R_4 = 1$  k $\Omega$ ,  $R_5 = 10$  M $\Omega$ , and  $R_6 \in [0.001, 1]$  M $\Omega$ . (b) Mean oscillation amplitude vs static stiffness  $V_{k0}$  plots under low amplitude  $V_{\Delta k} = 1$  V and high amplitude  $V_{\Delta k} = 2$  V parametric modulation. The same plot includes the static bifurcation diagram, i.e., equilibrium positions of the circuit under no parameter modulation, i.e.,  $V_{\Delta k} = 0$  V. The solid black lines (dashed gray lines) correspond to the behavior of the system displayed under quasistatic forward (backward) sweep experiments. The error bars on these plots indicate 3 standard deviations. (c) Phase plots and (d) optimal parameter modulation shown for selected experiments.

(iii) bandwidth limited parametric excitation—due to the inherent power limitation that applies to any physical mechanism used to implement parameter modulation [24]. While the proposed controller is not immune to these

effects [16], its performance is not sensitively affected, provided the imperfections are reasonably small and the bandwidth of the parameter modulation is high compared to the bandwidth of the oscillations. As a matter of fact, as long as the bandwidth of the modulation is an order of magnitude higher than the bandwidth of the oscillations, our feedback controller will provide a suboptimal *model-free* alternative of the truly-optimal model-based controller.

*Conclusion.*— The idea to feedback the detected movement to the oscillator, to perform direct forcing or parameter modulation, has been a central theme in many recent investigations [9–13]. Common to these approaches is the continuous frequency and phase identification from past observations and the time delay in the feedback loop used in the underlying delay feedback control implementation [8]. As an alternative idea, here we propose a discrete state feedback control scheme that implements an adaptive resonance condition while converting the original system to a hybrid state automaton.

We envision the present findings to be useful in generating robust large amplitude oscillations in a wide range of applications, including (i) microcantilevers used for mechanical domain per amplification in sensing applications (atomic force microscopy [25,26]), (ii) nanoelectromechanical resonators used as frequency determining elements (scaled-down alternatives to quartz crystals [27]) in timing applications [28], as well as (iii) large scale networks of electromechanical circuit resonators built to investigate the complexity of the human brain [29] through neurocomputation [30,31].

This work was supported by the author's Startup Research Grant (SRG-EPD-2014-074) at the Singapore University of Technology and Design. The author also thanks Dewmini Sudara (University of Moratuwa, Sri Lanka) for the development of the experimental setup used in this Letter.

---

\*david\_braun@sutd.edu.sg

- [1] M. Faraday, *Phil. Trans. R. Soc. London* **121**, 299 (1831).
- [2] É. Mathieu, *J. Math. Pure Appl.* **13**, 137 (1868).
- [3] L. Rayleigh, *Philos. Mag.* **15**, 229 (1883).
- [4] L. I. Mandelstam and N. D. Papaleksi, *J. Tech. Phys.* **4**, 5 (1934).
- [5] A. Nayfeh and D. Mook, *Nonlinear Oscillations* (Wiley-Interscience, New York, 1979).
- [6] W. Zhang, R. Baskaran, and K. L. Turner, *Sens. Actuator A-Phys.* **102**, 139 (2002).
- [7] J. F. Rhoads and S. W. Shaw, *Appl. Phys. Lett.* **96**, 234101 (2010).
- [8] K. Pyragas, *Phys. Lett. A* **170**, 421 (1992).
- [9] Y.-C. Lai, A. Kandangath, S. Krishnamoorthy, J. A. Gaudet, and A. P. S. de Moura, *Phys. Rev. Lett.* **94**, 214101 (2005).
- [10] D. Ramos, J. Mertens, M. Calleja, and J. Tamayo, *Appl. Phys. Lett.* **92**, 173108 (2008).
- [11] L. G. Villanueva, R. B. Karabalin, M. H. Matheny, E. Kenig, M. C. Cross, and M. L. Roukes, *Nano Lett.* **11**, 5054 (2011).
- [12] R. van Leeuwen, D. M. Karabacak, S. H. Brongersma, M. Crego-Calama, H. S. J. van der Zant, and W. J. Venstra, *Microelectron. Eng.* **98**, 463 (2012).
- [13] J. Gieseler, B. Deutsch, R. Quidant, and L. Novotny, *Phys. Rev. Lett.* **109**, 103603 (2012).
- [14] N. Minorsky, *J. Appl. Phys.* **22**, 49 (1951).
- [15] L. Pontryagin, V. Boltyanskii, R. Gamkrelidze, and E. Mishchenko, *The Mathematical Theory of Optimal Processes* (John Wiley and Sons, Inc., New York, 1962).
- [16] See Supplemental Material at <http://link.aps.org/supplemental/10.1103/PhysRevLett.116.044102>, which includes Ref. [17].
- [17] C. M. Bender and S. A. Orszag, *Advanced Mathematical Methods for Scientists and Engineers I* (Springer-Verlag, New York, 1999).
- [18] E. Meissner, *Schweiz. Bauztg.* **72**, 95 (1918).
- [19] K. L. Turner, S. A. Miller, P. G. Hartwell, N. C. MacDonald, S. H. Strogatz, and S. G. Adams, *Nature (London)* **396**, 149 (1998).
- [20] G. Duffing, *Erzwungene Schwingungen bei Veränderlicher Eigenfrequenz* (F. Vieweg u. Sohn, Braunschweig, 1918).
- [21] C. P. Silva and A. M. Young, U.S. Patent No. 6127899 (2000).
- [22] J. Guckenheimer and P. Holmes, *Nonlinear Oscillations, Dynamical Systems and Bifurcations of Vector Fields* (Springer-Verlag, New York, 1983).
- [23] P. Horowitz and W. Hill, *The Art of Electronics* (Cambridge University Press, Cambridge, England, 1989).
- [24] D. J. Braun, F. Petit, F. Huber, S. Haddadin, P. van der Smagt, A. Albu-Schäffer, and S. Vijayakumar, *IEEE Trans. Robot.* **29**, 1085 (2013).
- [25] G. Binnig, C. F. Quate, and C. Gerber, *Phys. Rev. Lett.* **56**, 930 (1986).
- [26] G. Prakash, S. Hu, A. Raman, and R. Reifengerger, *Phys. Rev. B* **79**, 094304 (2009).
- [27] W. Marrison, *Bell Syst. Tech. J.* **27**, 510 (1948).
- [28] C. T.-C. Nguyen, *IEEE Trans. Ultrason. Ferroelectr. Freq. Control* **54**, 251 (2007).
- [29] G. Buzsáki and A. Draguhn, *Science* **304**, 1926 (2004).
- [30] F. C. Hoppensteadt and E. M. Izhikevich, *Phys. Rev. Lett.* **82**, 2983 (1999).
- [31] S.-B. Shim, M. Imboden, and P. Mohanty, *Science* **316**, 95 (2007).